New Insight into *Phaeodactylum tricornutum* Fatty Acid Metabolism. Cloning and Functional Characterization of Plastidial and Microsomal Δ12-Fatty Acid Desaturases[1][w]

Frédéric Domergue*, Patricia Spiekermann, Jens Lerchl[2], Christoph Beckmann, Oliver Kilian, Peter G. Kroth, Wilhem Boland, Ulrich Zähringer, and Ernst Heinz

Institut für Allgemeine Botanik, Universität Hamburg, Ohnhorststrasse 18, 22609 Hamburg, Germany (F.D., P.S., E.H.); BASF Plant Science GmbH, BPS–A30, D–67056 Ludwigshafen, Germany (J.L.); Fachbereich Biologie, Universität Konstanz, D–78457 Konstanz, Germany (O.K., P.K.); Max-Planck-Institut für Chemische Ökologie, Carl-Zeiss-Promenade 10, D–07745 Jena, Germany (C.B., W.B.); and Forschungszentrum Borstel, Parkallee 22, D–23845 Borstel, Germany (U.Z.)

In contrast to 16:3 plants like rapeseed (*Brassica napus*), which contain α-linolenic acid ($18:3^{\Delta9,12,15}$) and hexadecatrienoic acid ($16:3^{\Delta7,10,13}$) as major polyunsaturated fatty acids in leaves, the silica-less diatom *Phaeodactylum tricornutum* contains eicosapentaenoic acid (EPA; $20:5^{\Delta5,8,11,14,17}$) and a different isomer of hexadecatrienoic acid ($16:3^{\Delta6,9,12}$). In this report, we describe the characterization of two cDNAs having sequence homology to Δ12-fatty acid desaturases from higher plants. These cDNAs were shown to code for a microsomal and a plastidial Δ12-desaturase (PtFAD2 and PtFAD6, respectively) by heterologous expression in yeast (*Saccharomyces cerevisiae*) and *Synechococcus*, respectively. Using these systems in the presence of exogenously supplied fatty acids, the substrate specificities of the two desaturases were determined and compared with those of the corresponding rapeseed enzymes (BnFAD2 and BnFAD6). The microsomal desaturases were similarly specific for oleic acid ($18:1^{\Delta9}$), suggesting that PtFAD2 is involved in the biosynthesis of EPA. In contrast, the plastidial desaturase from the higher plant and the diatom clearly differed. Although the rapeseed plastidial desaturase showed high activity toward the ω9-fatty acids $18:1^{\Delta9}$ and $16:1^{\Delta7}$, in line with the fatty acid composition of rapeseed leaves, the enzyme of *P. tricornutum* was highly specific for $16:1^{\Delta9}$. Our results indicate that in contrast to EPA, which is synthesized in the microsomes, the hexadecatrienoic acid isomer found in *P. tricornutum* ($16:3^{\Delta6,9,12}$) is of plastidial origin.

Diatoms (Bacillariophyceae) represent a significant group of eukaryotic microalgae found in marine and freshwater habitats and in terrestrial environments. In ocean ecosystems, they are thought to be responsible for as much as 25% of the global primary productivity (Scala and Bowler, 2001). Furthermore, they play a key role in the biogeochemical cycling of silica because most of them are surrounded by a highly structured silica cell wall (Tréguer et al., 1995). The plastids of diatoms contain xanthophylls like fucoxanthin as the major accessory pigments for photosynthesis, which give these organisms their brownish color and their denomination as chromophytes (Bhaya and Grossman, 1991). Phylogenetically, diatoms are thought to have originated from the engulfment of a photoautotrophic eukaryotic cell, most probably an ancestor of the modern red algae, by a heterotrophic heterokont flagellate (McFadden, 2001). Because of this secondary endocytobiosis, the chromophytic plastids of diatoms are surrounded by four membranes and referred to as "complex plastids." The two inner membranes of the plastid are thought to represent the original envelope of the plastid, whereas the two outer ones most probably evolved from the plasma membrane of the first endosymbiont and the phagotrophic membrane of the host cell (Kroth and Strotmann, 1999). The transport of nuclear-encoded proteins into such plastids was shown to depend on multisignal presequences and to be a two-step process (Lang et al., 1998).

The object of this study, *Phaeodactylum tricornutum*, is a silica-less diatom mainly known as a potential source for the industrial production of eicosapentaenoic acid (EPA; $20:5^{\Delta5,8,11,14,17}$; Molina Grima et al., 1996). In the fatty acid profile of *P. tricornutum* shown in Figure 1, EPA (30%), palmitoleic acid ($16:1^{\Delta9}$; 26%), palmitic acid (16:0; 17%), hexadecatrienoic acid ($16:3^{\Delta6,9,12}$; 10%), and myristic acid (14:0; 5%) are the major fatty acids. The first data concerning the fatty
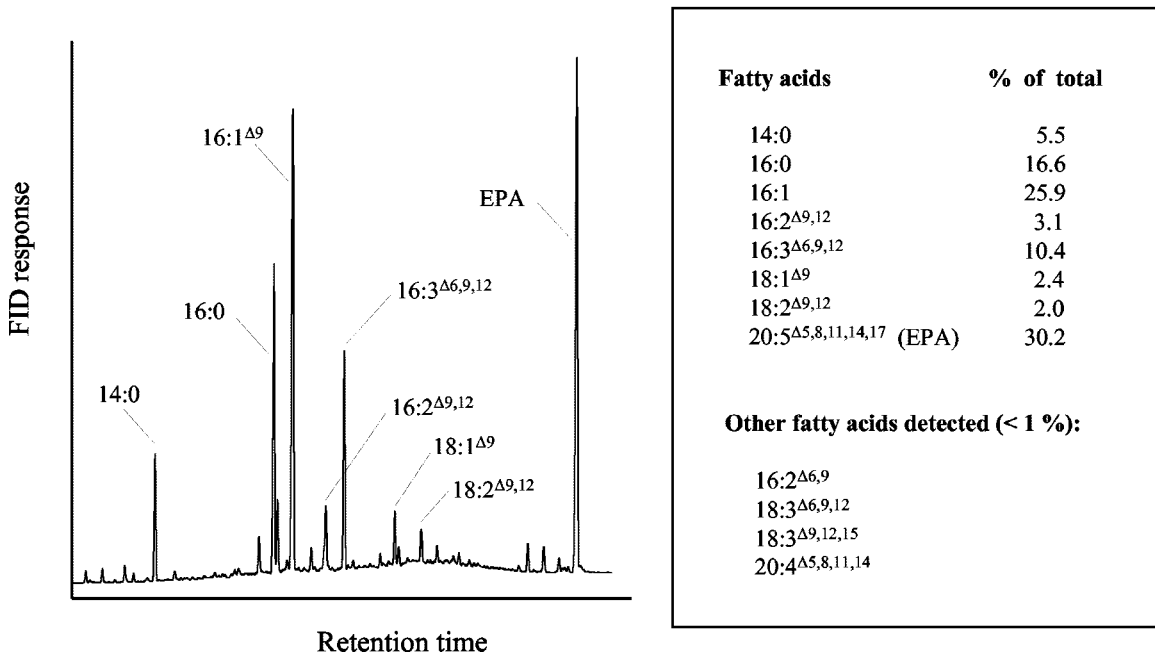
Fatty acids	% of total
14:0	5.5
16:0	16.6
16:1	25.9
$16:2^{\Delta9,12}$	3.1
$16:3^{\Delta6,9,12}$	10.4
$18:1^{\Delta9}$	2.4
$18:2^{\Delta9,12}$	2.0
$20:5^{\Delta5,8,11,14,17}$ (EPA)	30.2

Other fatty acids detected (< 1 %):

$16:2^{\Delta6,9}$
$18:3^{\Delta6,9,12}$
$18:3^{\Delta9,12,15}$
$20:4^{\Delta5,8,11,14}$

Figure 1. Fatty acid composition of *P. tricornutum*. *P. tricornutum* UTEX 646 was grown in brackish water medium with moderate shaking (80 rpm) under long-day light conditions (15 h at 30 μE m^{-2} s^{-1}) at 23°C. Cells were harvested in the stationary phase and fatty acid methyl esters (FAMEs) from whole cells were prepared as indicated in "Materials and Methods."

acid metabolism of *P. tricornutum* were obtained from labeling experiments. Incubation of the diatom with [^{14}C]acetate suggested that palmitic and oleic acid are the main products of the de novo synthesis (Moreno et al., 1979). Incubation with C18 or C20-[^{14}C]fatty acids showed that EPA was synthesized by desaturation and elongation of oleic acid (Arao and Yamada, 1994). In Figure 1, oleic acid and all the intermediates of the EPA biosynthetic pathway ($18:2^{\Delta9,12}$, $18:3^{\Delta6,9,12}$, $20:3^{\Delta8,11,14}$, and $20:4^{\Delta8,11,14,17}$) are only present in trace amounts. This may indicate that this organism has developed highly efficient mechanisms to accumulate specifically EPA. Recently, we reported the cloning and characterization of the Δ5- and the Δ6-desaturases involved in EPA biosynthesis in *P. tricornutum* (Domergue et al., 2002). Both desaturases are microsomal enzymes, which indicates that several steps involved in EPA biosynthesis are taking place in the endoplasmic reticulum (ER). On the other hand, most of the EPA found in *P. tricornutum* is present in the plastidial glycolipids (Arao et al., 1987; Yongmanitchai and Ward, 1993), suggesting an import of EPA into the plastid after its synthesis in the ER. Although the subcellular origin of EPA appears to be microsomal, that of the hexadecatrienoic acid isomer found in *P. tricornutum*, $16:3^{\Delta6,9,12}$, remains unclear.

In contrast to the fatty acid metabolism of diatoms, that of higher plants is well documented. In higher plants, the de novo fatty acid synthesis is catalyzed in the plastid by a type II (dissociable) fatty acid synthase, leading primarily to the synthesis of 16:0-ACP.

Most of this 16:0-ACP is then elongated to 18:0-ACP and desaturated to $18:1^{\Delta9}$-ACP by a soluble Δ9-acyl-ACP desaturase. Genetic and biochemical analyses of mutants of the model plant Arabidopsis have shown that two interconnected pathways are then responsible for the synthesis of $16:3^{\Delta7,10,13}$ and $18:3^{\Delta9,12,15}$, the two major polyunsaturated fatty acids (PUFAs) found in the leaves of 16:3 plants like Arabidopsis and rapeseed (*Brassica napus*; Browse and Somerville, 1991; Wallis and Browse, 2002). The so-called "eukaryotic" pathway is located in the ER and involved in the synthesis of $18:2^{\Delta9,12}$ and α-linolenic acid, $18:3^{\Delta9,12,15}$. In the chloroplast, the "prokaryotic" pathway catalyzes similar reactions, but is also responsible for the entire synthesis of the hexadecatrienoic acid isomer, $16:3^{\Delta7,10,13}$. Each pathway possesses its own set of Δ12- and Δ15-fatty acid desaturases (FADs), but they differ in both lipid substrates and electron donors. Although the plastidial desaturases of the prokaryotic pathway use primarily glycolipids as acyl-carriers and ferredoxin/ferredoxin oxidoreductase as electron donors, the microsomal desaturases involved in the eukaryotic pathway use phospholipids and cytochrome b5/cytochrome b5 oxidoreductase (Los and Murata, 1998). Such parallel sets of FADs may also exist in the plastidial and ER compartments of diatoms, and the cloning and functional characterization of these activities should help in understanding the origin of the predominating fatty acids found in *P. tricornutum*.

In the present paper, we report the cloning of two Δ12-FADs from *P. tricornutum* and their functional

characterization as microsomal and plastidial desaturase by expression in yeast (*Saccharomyces cerevisiae*) and a cyanobacterium, respectively. The substrate specificity of each desaturase was determined in these heterologous expression systems and compared with those of the corresponding homologs from rapeseed. The microsomal desaturase of *P. tricornutum* was shown to be most active with oleic acid, whereas the plastidial desaturase was highly specific for 16:1$^{\Delta 9}$. It could be concluded from these experiments that the microsomal desaturase is most probably involved in the biosynthesis of EPA, whereas the plastidial enzyme contributes to the synthesis of the hexadecatrienoic acid isomer characteristic to *P. tricornutum*, 16:3$^{\Delta 6,9,12}$, which in contrast to EPA, is most probably of prokaryotic origin.

RESULTS

Isolation of Two Δ12-Desaturase cDNA Clones

Two full-length clones coding for putative Δ12-desaturases were isolated from a *P. tricornutum* cDNA library by mass sequencing. The first clone was 1,651 bp long and contained an open reading frame (ORF) of 1,488 bp, which encoded a polypeptide of 495 amino acids. The second clone was 1,526 bp long, with an ORF of 1,311 bp coding for a polypeptide of 436 amino acids. The two proteins encoded by these ORFs were 28% identical (42%

similar), and both showed high sequence similarities to Δ12-desaturases from various organisms, including the rapeseed ω6-desaturase (BnFAD2; GenBank accession no. AF243045). This latter was 25% identical (38% similar) to the first *P. tricornutum* clone and 35% identical (49% similar) to the second one. When the N-terminal amino acid sequences were analyzed for the presence of targeting signals (Emanuelsson et al., 2000), the protein encoded by the first clone was predicted to be of plastidial origin. With respect to the nomenclature developed for such enzymes in Arabidopsis (Falcone et al., 1994; Okuley et al., 1994), the first and second ORFs identified in *P. tricornutum* were annotated as *PtFAD6* and *PtFAD2*, respectively.

Figure 2 shows the amino acid sequences of the proteins encoded by PtFAD2 and PtFAD6 together with the plastidial and microsomal homologs from rapeseed (BnFAD6 and BnFAD2, respectively). All these proteins contain the three conserved His clusters most likely involved in the coordination of the diiron center of the active site (Shanklin and Cahoon, 1998) and the four potential transmembrane helices of the topological model developed for membrane-bound desaturases (Shanklin et al., 1994). Both FAD6 proteins contain an N-terminal extension, the one of PtFAD6 being longer, as expected for the bipartite structure of the presequence encountered in diatoms (Lang et al., 1998).

Figure 2. Amino acid sequences of PtFAD6 and PtFAD2 in comparison with the plastidial and microsomal homologs from rapeseed. For alignment, the ClustalX program (Thompson et al., 1997) was used (gap opening 12, gap extension 0.05). The conserved amino acids are on gray background. The three His boxes are indicated by subscripts, and the potential transmembrane domains are framed. The broken line, dots, and the arrow at the N terminus of PtFAD6 indicate an hydrophobic domain, hydroxylated fatty acids (Thr and Ser), and the N-terminal sequence of PtFAD6 fused to EGPF, respectively. The sequence data from *P. tricornutum* have been submitted to the DNA Data Bank of Japan/EMBL/GenBank sequence data bank (accession nos. AY165023 and AY165024 for PtFAD2 and PtFAD6, respectively).
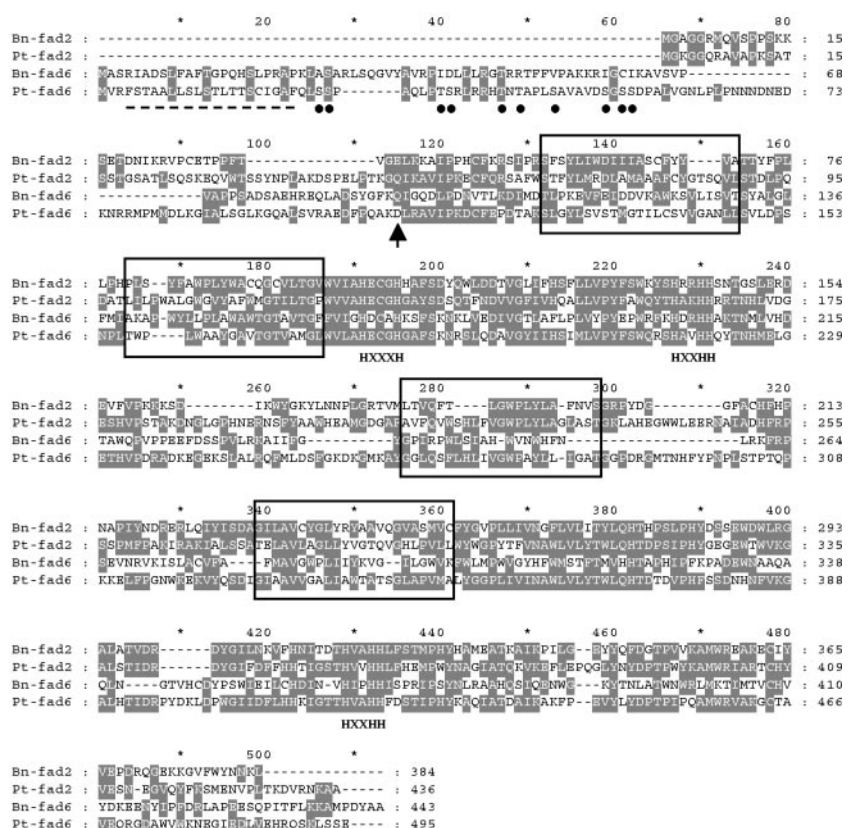
Presequence Analysis and Expression of Enhanced Green Florescent Protein (EGFP) Fusion Proteins

The presequence of PtFAD6 contains the two domains that are typical for the import of nuclear-encoded proteins into the complex plastids of diatoms. The N-terminal domain of PtFAD6 is basic with an Arg in the third position and contains a hydrophobic portion (Fig. 2, broken line) similar to a classical ER-targeting signal. This sequence is followed by a domain rich in hydroxylated amino acids (Ser and Thr; Fig. 2, dots), which is characteristic for transit peptides involved in the transport into the plastid.

To confirm the cellular localization of PtFAD6, the DNA sequence encoding the first 113 amino acids (Fig. 2, arrow) was fused with the EGFP gene and cloned in pPha-T1. The resulting vector was used to transform *P. tricornutum* (see "Materials and Methods"). As shown in Figure 3, the EGFP fluorescence was colocalized with the red fluorescence of chlorophyll in the plastid. Although the EGFP fluorescence was not evenly distributed within the plastid, but most probably accumulated within the pyrenoid, these results strongly support that PtFAD6 is a plastidial desaturase. In contrast, when the first 55 amino acids of PtFAD2 were fused to the N terminus of EGFP, the fluorescence appeared to be cytoplasmic (data not shown).

Functional Expression of the Desaturases in Yeast

The ORF of the putative microsomal desaturase PtFAD2 was cloned in the yeast expression vector pYES2 (Invitrogen, Leek, Netherlands) and expressed in yeast to confirm its enzymatic activity. Using the empty vector pYES2 as control and pYES2-*BnFAD2* for comparison, the different constructs were transformed into the yeast strain C13ABYS86 (Bröker et al., 1991) and expressed for 48 h at 20°C. The yeast cells transformed with the empty vector pYES2 showed the typical yeast fatty acids (16:0, 16:1$^{\Delta 9}$, 18:0, and 18:1$^{\Delta 9}$) and traces of 17:0 and 17:1$^{\Delta 9}$ (Fig. 4A, top). The expression of PtFAD2 and BnFAD2 resulted in two additional peaks corresponding to 16:2$^{\Delta 9,12}$ and 18:2$^{\Delta 9,12}$ (Fig. 4A, middle and bottom, respectively). The high proportions of 18:2$^{\Delta 9,12}$ were correlated with a significant decrease of 18:1$^{\Delta 9}$ as expected for an educt-product relation-
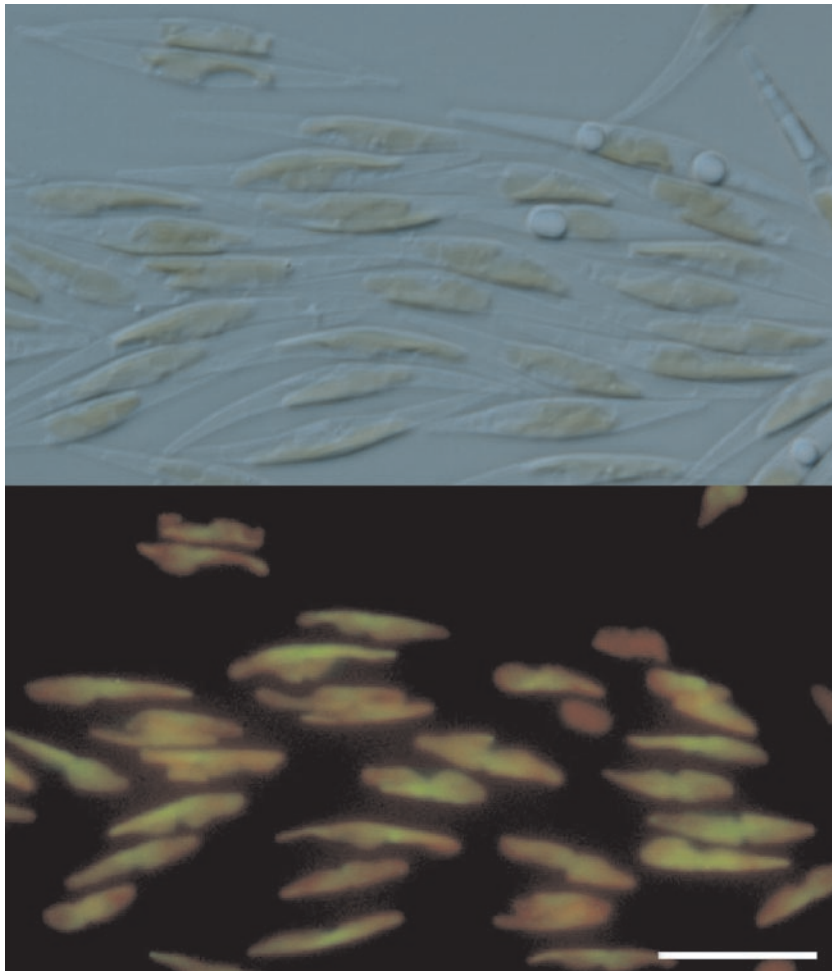
Figure 3. Expression of the PtFAD6-EGFP fusion protein in *P. tricornutum.* The DNA sequence encoding the first 113 amino acids of PtFAD6 was fused to the 5' end of the EGFP gene and cloned in pPha-T1. The resulting vector was used to transform *P. tricornutum* UTEX 646 as indicated in "Materials and Methods." Top, Light microscopical image of *P. tricornutum* with the plastids visible in brown. Bottom, Red (chlorophyll) and green (EGFP) fluorescence. Scale bar = 10 μm.

A
Microsomal desaturases

B
Plastidial desaturases
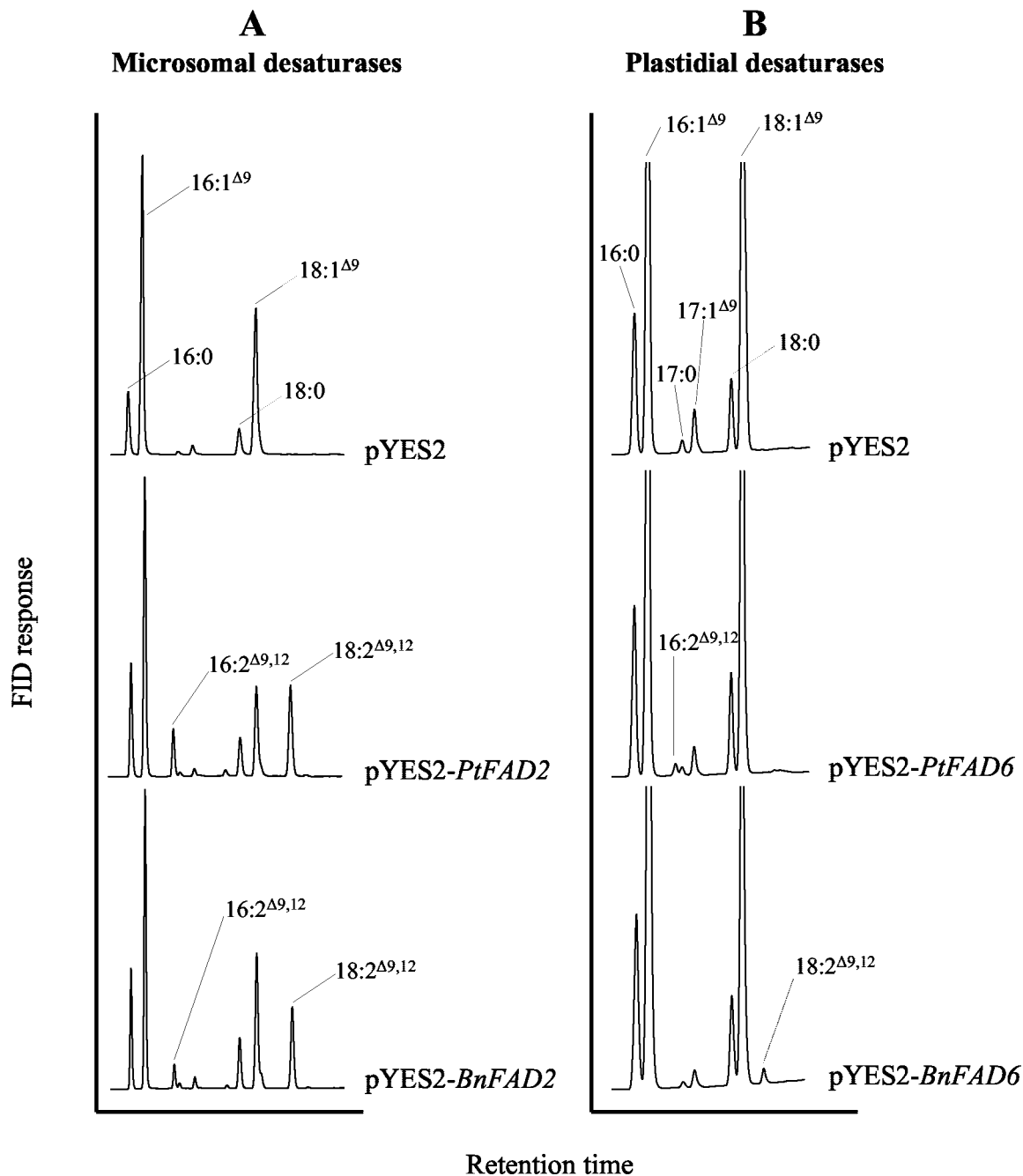
Figure 4. Fatty acid profiles of transgenic yeast expressing microsomal (A) and plastidial (B) desaturases. The C13ABYS86 yeast strain was transformed with the indicated constructs. The transformants were grown for 48 h at 20°C, and FAMEs from whole cells were prepared and analyzed by gas-liquid chromatography (GLC) as indicated in "Materials and Methods." The traces in B were magnified to show the small peaks representing the products of the plastidial desaturases, with the consequence that the peaks corresponding to $16:1^{\Delta 9}$ and $18:1^{\Delta 9}$ go off scale.

ship. PtFAD2 desaturated as much as 51% of oleic acid and about 14% of palmitoleic acid, whereas BnFAD2 was slightly less active, converting 40% and 8% of oleic and palmitoleic acid, respectively.

The yeast expression system was then used to determine the substrate specificity of PtFAD2 in more detail. The most efficiently desaturated substrate was oleic acid (50% conversion), but $16:1^{\Delta 9}$ and $17:1^{\Delta 9}$

were also accepted as substrates (15% and 22% conversion to $16:2^{\Delta 9,12}$ and $17:2^{\Delta 9,12}$, respectively; Table I). No activity was measured with $18:1^{\Delta 11}$ or $22:1^{\Delta 13}$, but about 4% of $20:1^{\Delta 11}$ was converted to $20:2^{\Delta 11,14}$. Similar results were obtained with BnFAD2 (data not shown), indicating that PtFAD2 has the substrate specificity typical for FAD2 enzymes. Although such enzymes can be denominated as ω6- or Δ12-

Table I. *Substrate specificity of PtFAD2 expressed in Saccharomyces cerevisiae*

Yeast strain C13ABYS86 transformed with pYES2-*PtFAD2* was grown for 48 h at 20°C in the presence or absence of different fatty acid substrates (500 μM or as indicated) in separate experiments. FAMEs from the whole cells were prepared and analyzed by GLC as indicated in "Materials and Methods." Each value represents the percent of total fatty acids and is the mean $\pm$ SD from three independent experiments. Desaturation (percentage) was calculated as (product $\times$ 100)/(educt + product).

Substrate	Total Fatty Acids (Educt)	Product	Total Fatty Acids	Desaturation
	%		%	%
[a]$16:1^{\Delta9}$	38.4 ± 1.6	$16:2^{\Delta9,12}$	6.6 ± 0.5	14.7
[b]$17:1^{\Delta9}$	2.9 ± 0.2	$17:2^{\Delta9,12}$	0.8 ± 0.1	22.3
[a]$18:1^{\Delta9}$	15.9 ± 1.1	$18:2^{\Delta9,12}$	16.1 ± 0.9	50.3
$18:1^{\Delta11}$	36.6 ± 2.2	$18:2^{\Delta11,14}$	0	0
[c]$20:1^{\Delta11}$	9.5 ± 0.9	$20:2^{\Delta11,14}$	0.4 ± 0.1	4.1
[c]$22:1^{\Delta13}$	2.0 ± 0.3	$22:2^{\Delta13,16}$	0	0

[a] In the absence of exogenously fed fatty acid. [b] In the presence of 2 mM exogenously fed 17:0. [c] In the presence of 2 mM exogenously fed fatty acid.

desaturases, it should be noted that they convert $16:1^{\Delta9}$ to $16:2^{\Delta9,12}$, $17:1^{\Delta9}$ to $17:2^{\Delta9,12}$, and $20:1^{\Delta11}$ to $20:2^{\Delta11,14}$ (Table I), inserting the new double bond in the ω4-, ω5-, and ω6/Δ14-position, respectively. Therefore, a correct assignment of the regioselectivity for FAD2 enzymes would be μ + 3 because the position of the incipient double bond is determined relative to a preexisting double bond by placing it three carbons closer to the methyl end (Meesapyodsuk et al., 2000).

Interestingly, when the FAD6 desaturases from *P. tricornutum* and rapeseed were expressed in yeast, small but significant proportions of $16:2^{\Delta9,12}$ and $18:2^{\Delta9,12}$ were detected, respectively (Fig. 4B). Repeatedly, $16:2^{\Delta9,12}$ accounted for 0.5% to 1.5% of the total fatty acids when PtFAD6 was expressed, whereas $18:2^{\Delta9,12}$ represented up to 2% of the total fatty acids in yeast expressing BnFAD6. Yeast is known to be the model of choice for the functional characterization of microsomal FADs because it contains the short electron transport system required by such desaturases (i.e. cytochrome b5 and NADH-cytochrome b5 reductase). Nevertheless, the low desaturation levels evident from Figure 4B suggest that desaturases of plastidial origin, which usually require ferredoxin and NADPH-ferredoxin reductase, are supplied to some extent with reducing equivalents in yeast cells.

Functional Expression of the Desaturases in *Synechococcus* PCC 7942

For the functional characterization of the putative plastidial FADs, the *Synechococcus* R2-PIM8 strain was used as a heterologous expression system (Fig. 5). *Synechococcus* transformed with the empty vector pFP1 presented a rather simple fatty acid profile with 16:0, $16:1^{\Delta9}$, $18:1^{\Delta9}$, and $18:1^{\Delta11}$ as the major fatty acids, whereas 18:0 was present in trace amounts (Fig. 5, top). When *Synechococcus* had been transformed with pFP1-*PtFAD2*, the fatty acid profile did not change, indicating that the microsomal desaturase was not active in the cyanobacterium. In con-

trast, transformation with pFP1-*BnFAD6* resulted in the expression of an active desaturase as indicated by the presence of three new fatty acids (Fig. 5, middle) corresponding to $16:2^{\Delta9,12}$, $18:2^{\Delta9,12}$, and $18:2^{\Delta11,14}$ as characterized by GLC-MS analysis of the 4,4-dimethyloxazoline derivatives. The expression of BnFAD6 resulted in the conversion of nearly all of the $18:1^{\Delta9}$ to $18:2^{\Delta9,12}$, whereas only a small proportion of $16:1^{\Delta9}$ was desaturated to $16:2^{\Delta9,12}$. The presence of $18:2^{\Delta11,14}$ could result either from the desaturation of $18:1^{\Delta11}$ or from the elongation of $16:2^{\Delta9,12}$, similar to the formation of $18:1^{\Delta11}$ from $16:1^{\Delta9}$. When PtFAD6 was expressed in *Synechococcus*, the same new fatty acids were detected but in different proportions (Fig. 5, bottom). $18:2^{\Delta9,12}$ was present in a very low percentage, whereas $16:2^{\Delta9,12}$ and $18:2^{\Delta11,14}$ were highly accumulated at the expense of $16:1^{\Delta9}$ and $18:1^{\Delta11}$.

Substrate Specificity of FAD6 Desaturases

The data presented in Figure 5 suggest that the favorite substrates of PtFAD6 and BnFAD6 differed and were $16:1^{\Delta9}$ and $18:1^{\Delta9}$, respectively, in agreement with the results obtained in yeast (Fig. 4B). Nevertheless, the origin of $18:2^{\Delta11,14}$ remained unclear. To clarify the origin of $18:2^{\Delta11,14}$ and to determine the substrate specificity of each desaturase in more detail, transgenic *Synechococcus* cultures were supplemented with $16:1^{\Delta9}$, $18:1^{\Delta9}$, or $18:1^{\Delta11}$, and grown for 1 week before fatty acid analysis (Fig. 6). In *Synechococcus* that had been transformed with pFP1 as control (Fig. 6, top), exogenously supplied $16:1^{\Delta9}$ increased only slightly the $16:1^{\Delta9}$ and $18:1^{\Delta11}$ content, confirming that $18:1^{\Delta11}$ results from the elongation of $16:1^{\Delta9}$. The fact that supplying $16:1^{\Delta9}$ had only a slight impact on the fatty acid composition of *Synechococcus* wild type was probably due to the high proportion of the endogenous $16:1^{\Delta9}$ (about 35%) present in the wild-type strain. In contrast, the proportion of $18:1^{\Delta9}$, which represents only about 4% of the total fatty acids in the wild-type strain, was increased more than 7 times
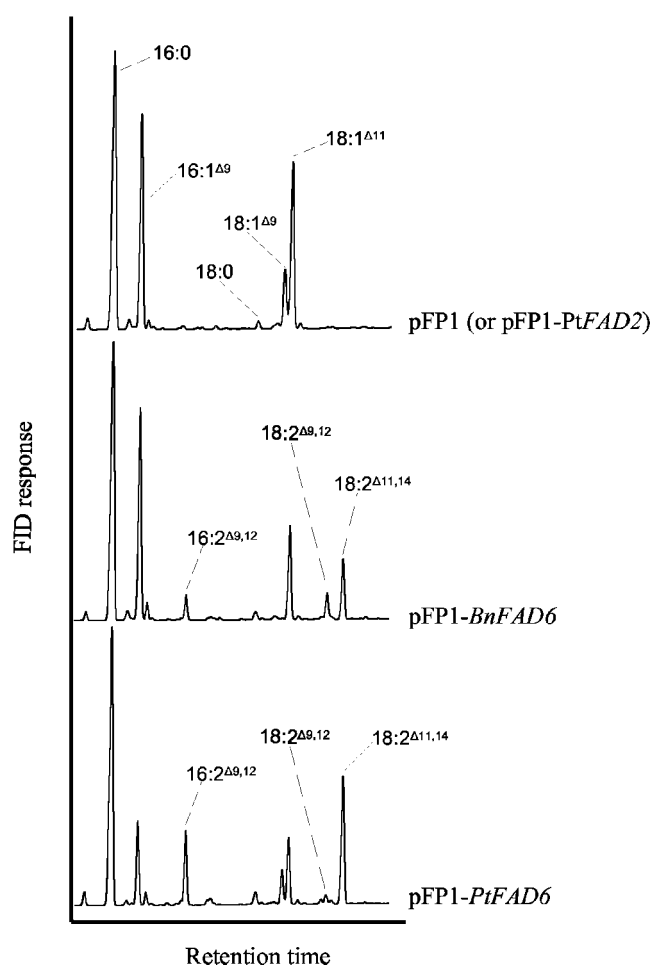
Figure 5. Fatty acid profiles of transgenic *Synechococcus* expressing plastidial desaturases. The *Synechococcus* R2-PIM8 strain was transformed with the indicated constructs. The transformants were grown at 23°C, and FAMEs from whole cells were prepared and analyzed by GLC as indicated in "Materials and Methods."

upon exogenous supply of $18:1^{\Delta 9}$. Finally, supplementing $18:1^{\Delta 11}$ doubled its proportion, reaching about 40% of the total fatty acids. In *Synechococcus* expressing BnFAD6 (Fig. 6, middle), exogenously supplied $16:1^{\Delta 9}$ barely changed the fatty acid composition, whereas supply of $18:1^{\Delta 9}$ resulted in a dramatic increase of $18:2^{\Delta 9,12}$, indicating that BnFAD6 had desaturated more than 87% of $18:1^{\Delta 9}$. In the presence of $18:1^{\Delta 11}$, the proportion of $18:1^{\Delta 11}$ was increased about 3 times but $18:2^{\Delta 11,14}$ remained nearly unchanged. When *Synechococcus* had been transformed with pFP1-*PtFAD6* (Fig. 6, bottom), supplementing $16:1^{\Delta 9}$ doubled the proportions of $18:1^{\Delta 11}$ but did not change that of $16:1^{\Delta 9}$, $16:2^{\Delta 9,12}$, or $18:2^{\Delta 11,14}$. In the presence of $18:1^{\Delta 9}$, although the proportion of $18:2^{\Delta 9,12}$ was increased, $18:1^{\Delta 9}$ accumulated to high levels, indicating that PtFAD6 had desaturated only 20% of the $18:1^{\Delta 9}$. When $18:1^{\Delta 11}$ was supplemented, the $18:2^{\Delta 11,14}$ percentage was lowered by about 50%, although the $18:1^{\Delta 11}$ proportion had been increased by more than 4 times, suggesting that $18:2^{\Delta 11,14}$ was

produced by elongation of $16:2^{\Delta 9,12}$ rather than by desaturation of $18:1^{\Delta 11}$. This was further supported by supplying exogenous $16:2^{\Delta 9,12}$ to *Synechococcus* transformed with pFP1. Although $16:2^{\Delta 9,12}$ was very poorly incorporated, 30% to 40% of it was converted to $18:2^{\Delta 11,14}$ in the absence of any Δ12-desaturase, confirming the presence in *Synechococcus* of an endogenous elongation activity converting $16:2^{\Delta 9,12}$ to $18:2^{\Delta 11,14}$. If we consider that none of the $18:2^{\Delta 11,14}$ was due to the action of PtFAD6 on $18:1^{\Delta 11}$, then more than 70% of $16:1^{\Delta 9}$ had been desaturated by PtFAD6.

The specificity of both desaturases was further evaluated by feeding other potential substrates for ω6-desaturation to the transgenic *Synechococcus* cultures (Table II). Both desaturases did not accept $22:1^{\Delta 13}$ as substrate, in contrast to previous data obtained in vitro for the plastidial desaturase from spinach (*Spinacia oleracea*; Schmidt and Heinz, 1993). Nevertheless, because the authors used an ω6-desaturase solubilized by Triton X-100 from chloroplast envelopes, the high activity with $22:1^{\Delta 13}$ obtained in this study may be artifactual and due to the presence of detergent in the assays. Similar to the FAD2 desaturases (Table I), BnFAD6 converted about 19% of $20:1^{\Delta 11}$ to $20:2^{\Delta 11,14}$, but PtFAD6 did not display activity toward that fatty acid. Because the plastidial desaturases of the 16:3 higher plants like rapeseed are involved in the synthesis of $16:3^{\Delta 7,10,13}$, $16:1^{\Delta 7}$ was chemically synthesized and tested as substrate. In *Synechococcus* transformed with pFP1, $16:1^{\Delta 7}$ accumulated to about 10% of the total fatty acids and was most probably not elongated to $18:1^{\Delta 9}$ because the content of oleic acid was not increased (data not shown). In the transgenic cyanobacteria expressing PtFAD6, only about 5% of $16:1^{\Delta 7}$ was converted to $16:2^{\Delta 7,10}$, whereas upon expression of BnFAD6, more than 80% of $16:1^{\Delta 7}$ was desaturated to $16:2^{\Delta 7,10}$ (Table II). The results presented in Table II clearly show that PtFAD6 is highly specific for $16:1^{\Delta 9}$, whereas BnFAD6 is as active with $16:1^{\Delta 7}$ as with $18:1^{\Delta 9}$, in line with its involvement in the synthesis of the two majors PUFAs of rapeseed leaves, $16:1^{\Delta 7,10,13}$ and $18:3^{\Delta 9,12,15}$. Similar to the microsomal desaturases, both plastidial enzymes display ω6 as well as ω4 activity, as already suggested by Hitz et al. (1994) for BnFAD6. It can be added that $16:1^{\Delta 7}$ was not accepted as substrate by the microsomal desaturases (PtFAD2 and BnFAD2) expressed in yeast (data not shown).

DISCUSSION

In this paper, we report the cloning and functional characterization of the microsomal and the plastidial Δ12-desaturase from the diatom *P. tricornutum*, PtFAD2 and PtFAD6, respectively. Similar to FADs from other species, both enzymes contain the three His clusters most likely coordinating the diiron center of the active site as well as long hydrophobic
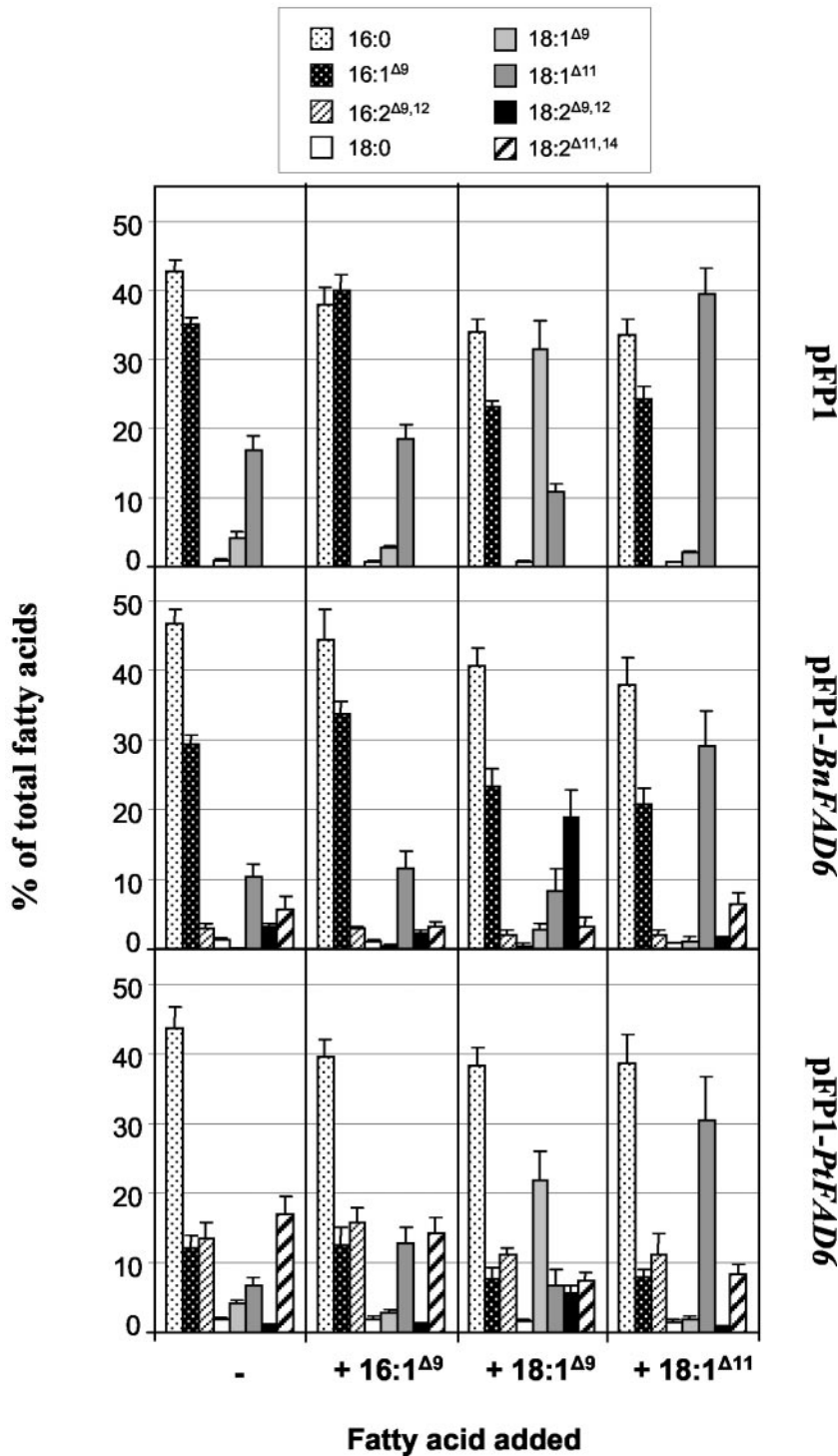
Figure 6. Fatty acid composition of transgenic *Synechococcus* expressing plastidial desaturases in the presence or absence of different exogenous fatty acids. The *Synechococcus* R2-PIM8 strain was transformed with the indicated constructs. The transformants were grown for a week at 23°C in the presence or absence of 75 μM 16:1$^{\Delta9}$, 18:1$^{\Delta9}$, or 18:1$^{\Delta11}$, and FAMEs from whole cells were prepared and analyzed by GLC as indicated in "Materials and Methods." Each value is the mean ± sd from three to five independent experiments.

stretches involved in membrane binding (Fig. 2; Shanklin et al., 1994). Although PtFAD2 presents moderate sequence homology to microsomal desaturases from higher plants (about 35% identity/50% homology), PtFAD6 has no homology to the corresponding plastidial desaturases (less than 14% identity/27% homology). As shown in the phylogenetic tree of desaturases presented in Figure 7, PtFAD2

and PtFAD6 form a separate branch between the microsomal desaturases from fungi (*Mucor rouxii* and *Mortierella alpina*) and another group containing the ω3- and ω6-desaturases of the nematode *Caenorhabditis elegans* (FAT1 and FAT2, respectively). The cyanobacterial Δ12-desaturase (DesA) groups together with the plastidial Δ12-desaturases from higher plants (Fig. 7) in line with the phylogenetic origin of

Table II. *Substrate specificity of the plastidial desaturases BnFAD6 and PtFAD6 expressed in Synechococcus*

Synechococcus was transformed with pFP1-*BnFAD6* or pFP1-*PtFAD6* and grown for 7 d at 23°C in the presence of different fatty acid substrates (75 μM) in separate experiments. FAMEs from the whole cells were prepared and analyzed by GLC as indicated in "Materials and Methods." Desaturation (percentage) was calculated as (product(s) $\times$ 100)/(educt + product(s)) using values corresponding to percent of total fatty acids. Each value is the mean $\pm$ SD from three to five independent experiments.

| Substrate	Product(s)	Desaturation	
		BnFAD6	PtFAD6
		%	
$16:1^{\Delta7}$	$16:2^{\Delta7,10}$	79.6 ± 5.8	5.2 ± 0.8
$16:1^{\Delta9}$	$16:2^{\Delta9,12}$, $18:2^{\Delta11,14a}$	15.5 ± 1.9	70.3 ± 3.1
$18:1^{\Delta9}$	$18:2^{\Delta9,12}$	87.3 ± 4.9	20.6 ± 2.5
$20:1^{\Delta11}$	$20:2^{\Delta11,14}$	19.4 ± 2.2	0
$22:1^{\Delta13}$	$22:2^{\Delta13,15}$	0	0

[a] Due to the endogenous elongation of the desaturase product $16:2^{\Delta9,12}$.

plastids. The large separation between DesA and PtFAD6 does not suggest that the latter one is derived from a cyanobacterial symbiont. On the other hand, it is accepted that a single primary endosymbiosis event represents the origin for the evolution of both the green (and the higher plants) and the red algae (Moreira et al., 2000). Because the evolution of diatoms is thought to have involved a secondary endocytobiosis, the plastidial desaturases from *P. tricornutum* may have a more complicated history. Because PtFAD6 is more similar to ER-localized desaturases, it could have evolved from the microsomal $\Delta12$-desaturase of the host of either the first or the second endosymbiosis. In the latter case, the gene of the microsomal desaturase of the heterotrophic flagellate that engulfed the photoautotrophic eukaryote could have been duplicated and the protein encoded by one copy redirected to the newly acquired plastid. A similar gene duplication may have given rise to the $\omega3$- and $\omega6$-desaturase of *C. elegans* (FAT1 and FAT2, respectively; Fig. 7) and is supported by the presence of conserved intron-exon junctions in both genes (Napier and Michaelson, 2001). Although the phylogenetic relationship of PtFAD2 and PtFAD6 looks similar to that of CeFAT1 and CeFAT2 in Figure 7, the two $\Delta12$-desaturases from *P. tricornutum* are much less similar and the absence of introns in the genomic sequences (data not shown) does not provide additional support for a similarly late gene duplication. It could also have happened that the gene of the microsomal $\Delta12$-desaturase from the ancestral red algae, the host of the first endosymbiont, has been transferred to the nuclear genome of the second host and that, after appropriate modifications, the product of its expression was targeted back to the first host, which during evolution became the complex plastid of *P. tricornutum*. Whatever the true origin of PtFAD6, these re-

sults are in agreement with the recent analysis of about 1,000 expressed sequence tags (ESTs) from *P. tricornutum*, which has shown that many sequences were more similar to animals than to plant counterparts, reflecting the different phylogenetic histories of diatoms and higher plants (Scala et al., 2002).

Because of their origin via secondary endocytobiosis, the plastids of the chromophytic diatoms are surrounded by four membranes. The transport of nuclear-encoded proteins into such complex plastids is a two-step process that relies on the bipartite structure of the targeting signal (Lang et al., 1998). The N-terminal sequence of the plastidial desaturase of *P. tricornutum* PtFAD6 (Fig. 2) contains a typical signal peptide for cotranslational transport through the ER membranes and a transit peptide for posttranslational protein targeting into the plastid. This bipartite presequence is sufficient to target EGFP into the plastid (Fig. 3). In contrast, fusing the N-terminal sequence of the microsomal desaturase PtFAD2 to EGFP led to cytoplasmic fluorescence (data not shown). In another study (Apt et al., 2002), the fusion of the N-terminal sequence of a lumenal protein to EGFP led to fluorescence within a network of membranes most probably representing the ER. In accordance, the N-terminal extremity of PtFAD2 preceding the first transmembrane domain (Fig. 2) seemed to contain no information for a localization within the microsomes. It should be added that the three microsomal desaturases from *P. tricornutum* characterized so far, PtFAD2 (this study), PtD5, and PtD6 (Domergue et al., 2002), do not contain the putative ER retention signal for diatoms, DDEL, at their C terminus. Immunocytological studies have shown that the FAD2 desaturases from higher plants are localized in the ER and face the cytosol (Dyer and Mullen, 2001). If PtFAD2 is similarly located in the ER, the information for its localization is most likely present within the transmembrane domains of the protein sequence.

The functional characterization of PtFAD2 and PtFAD6 in yeast and *Synechococcus*, respectively, confirmed that the former enzyme is a microsomal desaturase that uses cytochrome b5 and cytochrome b5 oxidoreductase as electron donors, whereas the latter desaturase is a plastidial protein requiring ferredoxin and ferredoxin oxidoreductase for electron donation. In addition, these heterologous expression systems enabled a detailed study of substrate specificities (Table I and II, respectively), which in turn led to a better understanding of the fatty acid metabolism in *P. tricornutum*. The clear preference of PtFAD2 for $18:1^{\Delta9}$ (50% conversion to $18:2^{\Delta9,12}$; Table I) fits with previous labeling experiments that had shown that EPA ($20:5^{\Delta5,8,11,14,17}$) was synthesized by desaturation and elongation of oleic acid (Arao and Yamada, 1994). Together with the recently cloned $\Delta5$- and $\Delta6$-desaturases (Domergue et al., 2002), PtFAD2 is the third microsomal enzyme involved in the biosynthesis of EPA to be characterized. It should be added
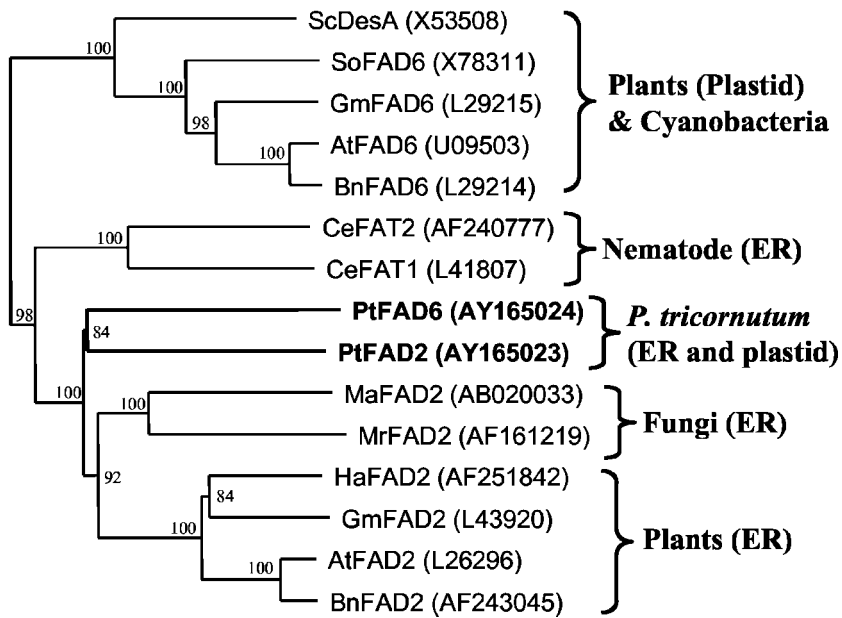
Figure 7. Phylogenetic tree of Δ12-desaturases from different organisms. The alignment was generated by the ClustalX program (Thompson et al., 1997), and the phylogenetic tree was constructed by the neighbor-joining method using Tree View (Page, 1996). Numbers indicate bootstrap values. The DNA Data Bank of Japan/EMBL/GenBank accession numbers of the different nucleic acid sequences coding for the desaturases used to construct this tree are indicated.

that the different intermediates of the EPA biosynthetic pathway were only present in trace amounts in the fatty acid profile obtained from *P. tricornutum* cells (Fig. 1) but found in much more abundant proportions in phospholipids, particularly in phosphatidylcholine (Arao et al., 1987). In contrast, the proportion of EPA was about the same in phosphatidylcholine, phosphatidylglycerol, and the total fatty acids (30%; Arao et al., 1987). From this, it may be concluded that in addition to the Δ12-, Δ6-, and Δ5-desaturation steps required for EPA biosynthesis, the Δ6-elongation and the ω3-desaturation steps are taking place in the microsomal fraction (Fig. 8). In contrast, the high specificity of PtFAD6 for $16:1^{\Delta 9}$ (Table II) suggests that $16:2^{\Delta 9,12}$ and most probably $16:3^{\Delta 6,9,12}$, the second major PUFA found in *P. tricornutum*, are synthesized within the plastid, similar to the hexadecatrienoic acid isomer found in 16:3 plants. Although $16:2^{\Delta 9,12}$ could leave the plastid, be converted to $16:3^{\Delta 6,9,12}$ by a microsomal Δ6-desaturase, and then re-incorporated into the plastid, this scenario seems unlikely. Because the microsomal Δ6-desaturase PtD6 is highly active with $18:2^{\Delta 9,12}$ but poorly active with both $16:1^{\Delta 9}$ (Domergue et al., 2002) and $16:2^{\Delta 9,12}$ (data not shown), we rather speculate that *P. tricornutum* contains a plastidial Δ6-desaturase that is involved in the synthesis of $16:3^{\Delta 6,9,12}$ (Fig. 8). It should be added that among the 3,860 ESTs that have been identified, no ESTs corresponding to an acyl-ACP desaturase, to a plastidial Δ6 desaturase, or to an ω3-desaturase were detected, and only one sequence having similarities to mammalian stearoyl-CoA desaturase was detected. Nevertheless, this clone was not full length and functionally characterized; therefore, its role in the fatty acid metabolism of *P. tricornutum* remains to be studied. In accordance, the number of Δ9-desaturases present in *P. tricornutum*

remains unclear: Is there a microsomal Δ9-desaturase specific for 18:0 and a plastidial Δ9-desaturase specific for 16:0, or is a single desaturase in the plastid responsible for the synthesis of both $16:1^{\Delta 9}$ and $18:1^{\Delta 9}$ as in cyanobacteria? Alternatively, a soluble Δ9-acyl-ACP desaturase and a membrane-bound Δ9-acyl-lipid desaturase, responsible for the synthesis of $18:1^{\Delta 9}$ and $16:1^{\Delta 9}$, respectively, could co-exist in the plastid of diatoms, similar to the situation found in higher plants.

Although the expression of a rapeseed FAD6 cDNA in *Synecchococcus* has already been achieved (Hitz et al., 1994), this is the first time, to our knowledge, that the substrate specificity of a plastidial desaturase is characterized in detail. The use of the *Synechococcus* R2-PIM8 strain as a heterologous expression system was instrumental in this, as evidenced by the high desaturation activities reported in Figures 5 and 6 and in Table II. These results confirm the strong activity of the *npt*II promoter in *Synechococcus* and demonstrate the usefulness of the R2-PIM8 strain for the functional characterization of plastidial enzymes involved in fatty acid metabolism. The substrate specificity of BnFAD6 reported in Table II confirms that the plastidial Δ12-desaturases of 16:3 plants are involved in the synthesis of the two trienoic fatty acids found in the leaves of such plants, $16:3^{\Delta 7,10,13}$ and $18:3^{\Delta 9,12,15}$. In addition, the high activity of the microsomal desaturase BnFAD2 with $18:1^{\Delta 9}$ (Fig. 4A) is in agreement with the involvement of this enzyme in the synthesis of $18:2^{\Delta 9,12}$ in the ER. In 16:3 plants like rapeseed, two glycerolipid biosynthetic pathways co-exist: The prokaryotic pathway in the plastid leads to the synthesis of glycolipids with $18:3^{\Delta 9,12,15}$ and $16:3^{\Delta 7,10,13}$ at the *sn*-1 and *sn*-2 position, respectively, whereas the eukaryotic pathway in
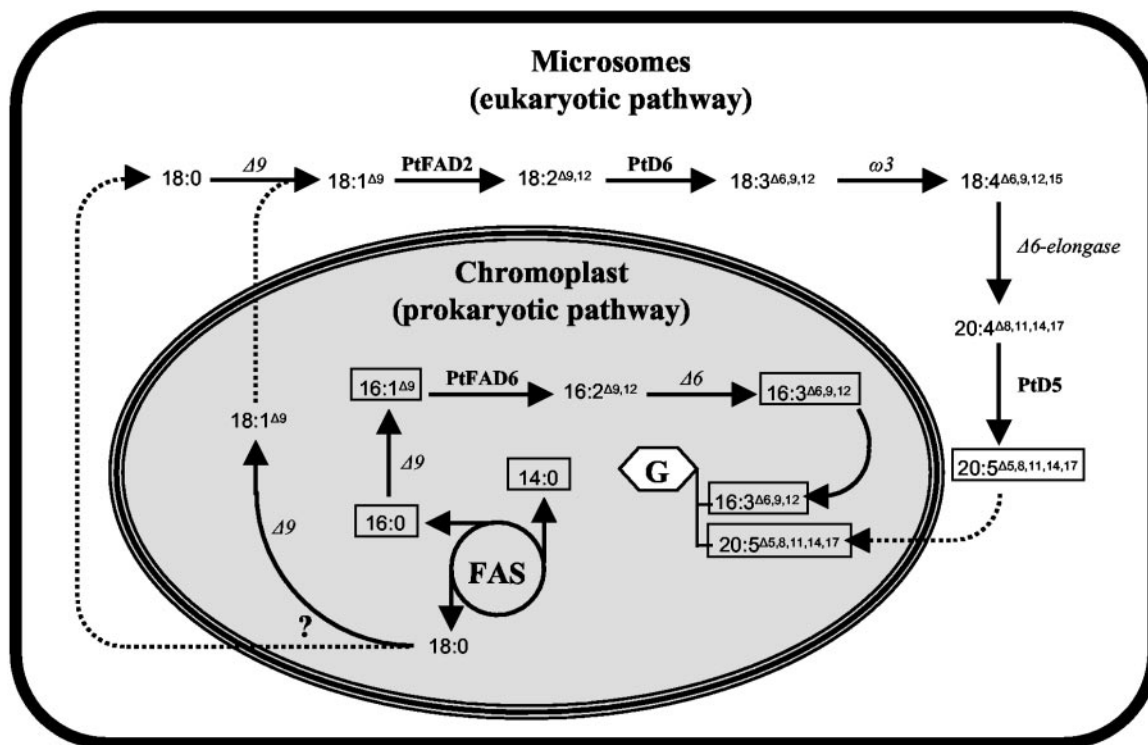
Figure 8. Hypothetical compartmentalization of fatty acid metabolism in *P. tricornutum* cells. The main fatty acids present in *P. tricornutum* (see Fig. 1) are framed. Desaturase genes that have been cloned are marked in bold, whereas putative desaturase ($\Delta6$, $\omega3$, and $\Delta9$) and elongase are indicated with italics. Fatty acid modifications are indicated by arrows, and possible exchange reactions are indicated by dashed lines. The backbone with the framed G refers to the major glycolipids found in the plastid of *P. tricornutum* (monogalactosyldiacylglycerol, digalactosyldiacylglycerol, and suphoquinovosyldiacylglycerol). Thioester- or lipid-linked desaturation is not differentiated and actually not known in detail. FAS, Fatty acid synthase.

the ER is contributing to the synthesis of glycolipids with $18:3^{\Delta9,12,15}$ at both positions (Browse and Somerville, 1991; Wallis and Browse, 2002). In *P. tricornutum*, the most abundant glycolipids contain EPA and unsaturated 16 carbon fatty acids at the *sn*-1 and *sn*-2 position, respectively (Fig. 8; Arao et al., 1987; Yongmanitchai and Ward, 1993), which is considered to be a typically prokaryotic diacylglycerol backbone. Such a denomination is nevertheless ambiguous in the case of *P. tricornutum* because the results presented in this study demonstrate that the 16 carbon fatty acids at the *sn*-2 position are most probably synthesized exclusively by a plastidial prokaryotic pathway, whereas EPA at the *sn*-1 position is of eukaryotic origin. Whether EPA is imported into the chromoplast of *P. tricornutum* as a free fatty acid in reversal of the fatty acid export from plastids, or whether it is linked to a glycerol backbone similar to the situation prevailing in higher plants, deserves further investigation. The lipid exchange between plastids and other compartments may differ to some extent regarding nature of intermediates and direction of transport when looking at organisms such as algae, which differ in fatty acid diversity from the monotonous situation encountered in higher plants.

MATERIALS AND METHODS

Materials

Restriction enzymes, polymerases, and DNA-modifying enzymes were obtained from New England BioLabs (Frankfurt) unless indicated otherwise. All other chemicals were from Sigma (St. Louis).

Culture of *Phaeodactylum tricornutum*

P. tricornutum UTEX 646 was grown in brackish water medium (Schlösser, 1993) at 23°C with moderate shaking under long-day light conditions (15 h at 30 μE m^{-2} s^{-1}). Cells were harvested by centrifugation, washed with water, and used for fatty acid analysis.

Isolation of *P. tricornutum* cDNA Clones

A *P. tricornutum* cDNA library was constructed and subjected to random sequencing as previously described (Domergue et al., 2002). Among the 3,860 nonredundant clones obtained, three sequences presented high homologies to various $\Delta12$-desaturases and were fully sequenced. Two clones originating from a single gene overlapped, but Pt001072031r and Pt001070010r differed and each contained a full-length ORF.

Isolation of Rapeseed *Brassica napus* cDNA Clones

Using an excised rapeseed cv Askari cDNA library as template and primers designed according to the sequences available in databases, clones corresponding to the rapeseed plastidial and microsomal desaturases

(*BnFAD6* and *BnFAD2*, respectively) were amplified by PCR and sequenced. The nucleotide sequences of the clones *BnFAD6* and *BnFAD2* presented in this study were 95% and 96% identical to that of the rapeseed plastidial ω6-desaturase (accession no. L29214) and that of the rapeseed Δ12-oleate desaturase (accession no. AF243045), respectively. The deduced proteins differed slightly from those already published (accession nos. AAF78778 and AAA50157). BnFAD2 presented three amino acid changes (T20N, A246V, and L266F) whereas BnFAD6 had eight substitutions at the N terminus (Q17H, C18S, P32Q, L53F, F66S, N76S, D79H, and E83D), respectively.

Functional Characterization in Yeast (*Saccharomyces cerevisiae*)

For functional characterization, the four desaturase sequences were cloned in the yeast expression vector pYES2 (Invitrogen). The ORFs of *BnFAD6*, *PtFAD2*, and *PtFAD6* were modified by PCR to create *Bam*HI and *Xho*I restriction sites adjacent to the start and stop codons, respectively, and to insert the yeast consensus sequence for enhanced translation (Donahue and Cigan, 1990) in front of the start codon. The ORF of *BnFAD2* was similarly amplified but with *Kpn*I and *Xba*I sites. All these PCR products were cloned into the pGEM-T vector (Promega, Madison, WI), and the ORFs were released by *Bam*HI/*Xho*I (or *Kpn*I/*Xba*I) digestion. Cloning of the *PtFAD2*, *PtFAD6*, *BnFAD2*, and *BnFAD6* ORFs in pYES2 using the same sites yielded pYES2-*PtFAD2*, pYES2-*PtFAD6*, pYES2-*BnFAD2*, and pYES2-*BnFAD6*, respectively.

Yeast strain C13ABYS86 (*leu2*, *ura3*, *his*, *pra1*, *prb1*, *prc1*, and *cps*; Bröker et al., 1991) was transformed with plasmid DNA by a modified polyethylene glycol/lithium acetate protocol (Ausubel et al., 1995). After selection on minimal medium agar plates without uracil, cells harboring the vector were cultivated in minimal medium lacking uracil but containing 2% (w/v) raffinose and 1% (v/v) Tergitol NP-40. Expression was induced by supplementing Gal to 2% (w/v) when the cultures had reached an A_{600} of 0.2 to 0.3. At that time, the appropriate fatty acids were added to a final concentration of 500 μM, unless indicated otherwise, and the cultures were further grown for 48 h at 20°C. Cells were harvested by centrifugation, and the pellet was washed once with 0.1 M NaHCO₃ before being used for fatty acid analysis.

Functional characterization in *Synechococcus*

The *Synechococcus* PCC7972 strain R2-PIM8, which contains an integration platform in the *metF* gene for pBR322-derived plasmids (van der Plas et al., 1990), was used to express the PtFAD2, PtFAD6 and BnFAD6 desaturases. For this purpose, the plasmid pFP1–3 (Götz et al., 1999) was digested with *Sma*I, dephosphorylated with the calf intestinal alkaline phosphatase, purified, and self-ligated, yielding the plasmid pFP1. The *PtFAD2*, *PtFAD6*, and *BnFAD6* ORFs were cut out of pYES2-*PtFAD2*, pYES2-*PtFAD6*, and pYES2-*BnFAD6*, respectively, by *Bam*HI/*Xho*I digestion, blunt ended with Klenow enzyme, and phosphorylated with T₄ polynucleotide kinase. Each ORF was then inserted in the correct orientation in pFP-1 opened with *Sma*I, yielding pFP1-*PtFAD2*, pFP1-*PtFAD6*, and pFP1-*BnFAD6*, respectively.

The *Synechococcus* R2-PIM8 strain was cultured in BG11 medium (Rippka et al., 1979) supplemented with 30 μg mL⁻¹ Met and 10 μg mL⁻¹ streptomycin at 23°C with moderate shaking and under long-day light conditions (15 h at 30 μE m⁻² s⁻¹). Transformation was conducted according to Windhövel et al. (1994), and transformants were selected on BG11 plates (1.5% [w/v] Bacto-agar) containing 30 μg mL⁻¹ Met, 1 μg mL⁻¹ ampicillin, and 10 μg mL⁻¹ kanamycin. When fatty acids were exogenously supplied, growing cultures were sedimented by centrifugation and resuspended in 30 mL of BG11 containing Met, ampicillin, kanamycin, and 75 μM fatty acid. The cultures were further grown for a week at 23°C, harvested by centrifugation, and the pellet was washed once with 0.1 M NaHCO₃ before being used for fatty acid analysis.

Fatty Acid Analysis

Cell sediments were directly transmethylated with 1 N sulfuric acid in methanol containing 2% (v/v) dimethoxypropane (1 h at 80°C) to prepare FAMEs. FAMEs were extracted in petroleum ether and analyzed by GLC as already described (Domergue et al., 2002). Fatty acids were identified by

comparison with appropriate reference substances or by GLC-MS of 4,4-dimethyloxazoline derivatives as described earlier (Sperling et al., 2000).

GFP Expression in *P. tricornutum*

The N-terminal part of the plastidial or the microsomal desaturase from *P. tricornutum* was fused to the N-terminus of EGFP. For this purpose, the first 165 and 339 bp of the ORF of PtFAD2 and PtFAD6, respectively, were cloned in frame at the 5′ end of the nucleotidic sequence coding for EGFP. The resulting EGFP fusions were inserted into the *P. tricornutum* transformation vector pPha-T1, and transformation of the diatom was achieved by microparticle bombardment (Zaslavskaia et al., 2000). Selection and culture of the transformants and light and fluorescence microscopy were carried out according to Apt et al. (2002).

Chemical Synthesis of 16:1^{Δ7} and 16:2^{Δ9,12}

The synthesis of (7Z)-hexadec-7-enoic acid (16:1^{Δ7}) was achieved by a cis-selective Wittig reaction (Bestmann et al., 1976) of 7-phosphoranylheptanoic acid methyl ester and nonanal in 40% (w/v) yield. (9Z,12Z)-hexadeca-9,12-dienoic acid (16:2^{Δ9,12}) was synthesized along a protocol described for the synthesis of homoconjugated trienoic acids (Pohnert and Boland, 2000; Zank et al., 2002). Successive treatment of the symmetrical bisphosphorane with butanal and methyl 9-oxononanoate, using a carefully optimized regime of temperatures, yielded the methyl ester of 16:2^{Δ9,12} in a single operation and 42% (w/v) yield. The free fatty acids were obtained by saponification of the respective methyl ester with LiOH in THF:water (3:1 [v/v]; Nicolaou et al., 1986).

Details of the syntheses and spectroscopic data are available as supplementary material (see www.plantphysiol.org for supplemental material).

LITERATURE CITED

Apt KE, Zaslavkaia L, Lippmeier JC, Lang M, Kilian O, Wetherbee R, Grossman AR, Kroth PG (2002) In vivo characterization of diatom multipartite plastid targeting signals. J Cell Sci **115:** 4061–4069

Arao T, Kawaguchi A, Yamada M (1987) Positional distribution of fatty acids in lipids of the marine diatom, *Phaeodactylum tricornutum*. Phytochemistry **26:** 2573–2576

Arao T, Yamada M (1994) Biosynthesis of polyunsaturated fatty acids in the marine diatom, *Phaeodactylum tricornutum*. Phytochemistry **35:** 1177–1181

Ausubel FM, Brent R, Kingston RE, Moore DD, Seidman JG, Smith JA, Struhl K, Albright LM, Coen DM, Varki A (1995) Current Protocols in Molecular Biology. John Wiley and Sons, New York

Bestmann HJ, Stransky W, Vostrowsky O (1976) Reactions of Alkylidenetriphenylphosphoranes: 33. Preparation of lithium salt-free ylid solutions with sodium bis(trimethylsilyl) amide as base. Chem Ber-Recl **109:** 1694–1700

Bhaya D, Grossman A (1991) Targeting proteins to diatom plastids involves transport through an endoplasmic reticulum. Mol Gen Genet **229:** 400–404

Bröker M, Bauml O, Gottig A, Ochs J, Bodenbenner M, Amann E (1991) Expression of the human blood coagulation protein factor XIIIa in *Saccharomyces cerevisiae*: dependence of the expression levels from host-vector systems and medium conditions. Appl Microbiol Biotechnol **34:** 756–764

Browse J, Somerville C (1991) Glycerolipid synthesis: biochemistry and regulation. Annu Rev Plant Physiol Plant Mol Biol **42:** 467–506

Domergue F, Lerchl J, Zähringer U, Heinz E (2002) Cloning and functional characterization of *Phaeodactylum tricornutum* front-end desaturases in-

volved in eicosapentaenoic acid biosynthesis. Eur J Biochem **269:** 4105–4113

Donahue TF, Cigan AM (1990) Sequence and structural requirements for efficient translation in yeast. Methods Enzymol **185:** 366–372

Dyer JM, Mullen RT (2001) Immunocytological localization of two plant fatty acid desaturases in the endoplasmic reticulum. FEBS Lett **494:** 44–47

Emanuelsson O, Nielsen H, Brunak S, von Heijne G (2000) Predicting subcellular localization of proteins based on their N-terminal amino acid sequence. J Mol Biol **300:** 1005–1016

Falcone DL, Gibson S, Lemieux B, Somerville C (1994) Identification of a gene that complements an *Arabidopsis* mutant deficient in chloroplast omega 6 desaturase activity. Plant Physiol **106:** 1453–1459

Götz T, Windhövel U, Böger P, Sandmann G (1999) Protection of photosynthesis against ultraviolet-B radiation by carotenoids in transformants of the cyanobacterium *Synechococcus* PCC7942. Plant Physiol **120:** 599–604

Hitz WD, Carlson TJ, Booth JR, Kinney AJ, Stecca KL, Yadav NS (1994) Cloning of a higher-plant plastid *ω*-6 fatty acid desaturase cDNA and its expression in a cyanobacterium. Physiol Plant **105:** 635–641

Kroth PG, Strotmann H (1999) Diatom plastids: secondary endocytobiosis, plastid genome and protein import. Physiol Plant **107:** 136–141

Lang M, Apt KE, Kroth PG (1998) Protein transport into "complex" diatom plastids utilizes two different targeting signals. J Biol Chem **273:** 30973–30978

Los DA, Murata N (1998) Structure and expression of fatty acid desaturases. Biochem Biophys Acta **1394:** 3–15

McFadden GI (2001) Primary and secondary endosymbiosis and the origin of plastids. J Phycol **37:** 951–959

Meesapyodsuk D, Reed DW, Savile CK, Buist PH, Ambrose SJ, Covello PS (2000) Characterization of the regiochemistry and cryptoregiochemistry of a *Caenorhabditis elegans* fatty acid desaturase (*FAT-1*) expressed in *Saccharomyces cerevisiae*. Biochemistry **39:** 11948–11954

Molina Grima E, Robles Medina A, Giménez Giménez A, Ibáñez González MJ (1996) Gram-scale purification of eicosapentaenoic acid (EPA, 20,5n-3) from wet *Phaeodactylum tricornutum* UTEX 640 biomass. J Appl Phycol **8:** 359–367

Moreira D, Le Guyader H, Philippe H (2000) The origin of red algae and the evolution of chloroplasts. Nature **405:** 69–72

Moreno VJ, De Moreno JEA, Brenner RR (1979) Biosynthesis of unsaturated fatty acids in the diatom *Phaeodactylum tricornutum*. Lipids **14:** 15–19

Napier JA, Michaelson LV (2001) Genomic and functional characterization of polyunsaturated fatty acid biosynthesis in *Caenorhabditis elegans*. Lipids **36:** 761–766

Nicolaou KC, Ladduwahetty T, Taffer IM, Zipkin RE (1986) A general strategy for the synthesis of monohydroxyeicosatetraenoic acids: total synthesis of 5(S)-hydroxy-6(E),8,11,14(Z)-eicosatetraenoic acid (5-Hete) and 12(S)-hydroxy-5,8,14(Z),10(E)-eicosatetraenoic acid (12-Hete). Synthesis 344–347

Okuley J, Lightner J, Feldmann K, Yadav N, Lark E, Browse J (1994) *Arabidopsis* FAD2 gene encodes the enzyme that is essential for polyunsaturated lipid synthesis. Plant Cell **6:** 147–158

Page R (1996) Tree View: an application to display phylogenic trees on personal computers. Comput Appl Biosci **12:** 357–358

Pohnert G, Boland W (2000) Highly efficient one-pot double-Wittig approach to unsymmetrical (1Z,4Z,7Z)-homoconjugated trienes. Eur J Org Chem **9:** 1821–1826

Rippka R, Deruelles J, Waterbury JB, Herdman M, Stanier RY (1979) Generic assignments, strain histories and properties of pure cultures of cyanobacteria. J Gen Microbiol **111:** 1–61

Scala S, Bowler C (2001) Molecular insights into the novel aspects of diatom biology. Cell Mol Life Sci **58:** 1666–1673

Scala S, Carels N, Falciatore A, Chiusano ML, Bowler C (2002) Genome properties of the diatom *Phaeodactylum tricornutum*. Plant Physiol **129:** 993–1002

Schlösser UG (1993) SAG-Sammlung von Algenkulturen at the University of Göttingen: catalogue of strains 1994. Bot Acta **107:** 113–186

Schmidt H, Heinz E (1993) Direct desaturation of intact galactolipids by a desaturase solubilized from spinach (*Spinacia oleracea*) chloroplast envelopes. Biochem J **289:** 777–782

Shanklin J, Cahoon EB (1998) Desaturation and related modifications of fatty acids. Annu Rev Plant Physiol Plant Mol Biol **49:** 611–641

Shanklin J, Whittle E, Fox BG (1994) Eight histidine residues are catalytically essential in a membrane-associated iron enzyme, stearoyl-CoA desaturase, and are conserved in alkane hydroxylase and xylene monooxygenase. Biochemistry **33:** 12787–12794

Sperling P, Lee M, Girke T, Zähringer U, Stymne S, Heinz E (2000) A bifunctional delta 6-fatty acyl acetylenase/desaturase from the moss *Ceratodon purpureus*: a new member of the cytochrome b5 superfamily. Eur J Biochem **267:** 3801–3811

Thompson JD, Gibson TJ, Plewniak F, Jeanmougin F, Higgins DG (1997) The CLUSTAL X windows interface: flexible strategies for multiple sequence alignment aided by quality tools. Nucleic Acids Res **25:** 4876–4882

Tréguer P, Nelson DM, Van Bennekom AJ, De Master D, Leynaert A, Quéguiner B (1995) The silica balance in the world ocean: a reestimate. Science **268:** 375–379

van der Plas J, Hegeman H, de Vrieze G, Tuyl M, Borrias M, Weisbeek P (1990) Genomic integration system based on pBR322 sequences for the cyanobacterium *Synechococcus* sp. PCC7942: transfer of genes encoding plastocyanin and ferredoxin. Gene **95:** 39–48

Wallis JG, Browse J (2002) Mutants of *Arabidopsis* reveal many roles for membrane lipids. Prog Lipid Res **41:** 254–278

Windhövel U, Geiges B, Sandmann G, Böger P (1994) Expression of *Erwinia uredovora* phytoene desaturase in *Synechococcus* PCC7942 leading to resistance against a bleaching herbicide. Plant Physiol **104:** 119–125

Yongmanitchai W, Ward OP (1993) Positional distribution of fatty acids, and molecular species of polar lipids, in the diatom *Phaeodactylum tricornutum*. J Gen Microbiol **139:** 465–472

Zank TK, Zähringer U, Beckmann C, Pohnert G, Boland W, Holtorf H, Reski R, Lerchl J, Heinz E (2002) Cloning and functional characterisation of an enzyme involved in the elongation of delta6-polyunsaturated fatty acids from the moss *Physcomitrella patens*. Plant J **31:** 255–268

Zaslavskaia LA, Lippmeier JC, Kroth PG, Grossman AR, Apt KE (2000) Transformation of the diatom *Phaeodactylum tricornutum* (Bacillariophyceae) with a variety of selectable marker and reporter genes. J Phycol **36:** 379–986